OMEGA-CRISM Characterization of Mafic Crustal Composition: Pyroxene. J. F. Mustard[1], P. Thollot[1], S. L. Murchie[2], S. M. Pelkey[1], B. L. Ehlmann[1], L. A. Roach[1], F. Seelos[2], F. Poulet[3], J.-P. Bibring[3], and the CRISM science team. [1]Dept. of Geological Sciences, Box 1846, Brown University, Providence, RI 02912 John_Mustard@brown.edu, [2]JHU/Applied Physics Laboratory, Laurel, MD 20723, [3]Institute d'Astrophysique Spatial, Université Paris 11, 91405 Orsay Cedex, France.

Introduction: The mafic mineralogy of the martian crust records crust forming processes and the composition of melt source regions associated with volcanism. A variety of sources of information about the igneous composition of the martian crust have been examined including remotely sensed data, meteorites, and in situ observations by landers and rovers [1]. While meteorites exhibit the greatest petrologic diversity, most of the samples are <1.3 Ga in age and thus young relative to the majority of the Mars surface. Remotely sensed and landed measurements are dominated by the signatures of feldspar, pyroxene, and olivine and imply that, where exposed, the igneous crust is dominantly basaltic [2, 3]. Global analysis of thermal infrared data (TIR) identified two major divisions in crustal composition. Type I material, predominantly in the equatorial highlands, is basaltic, and Type II, found predominantly in the northern lowland plains, has been variously interpreted to be andesite or basaltic andesite [4], altered basalt with a significant component of hydrolytic weathering materials [5,6], oxidized basalt [7] or silica-coated basalt [8].

Here we present the first results for the crustal composition of Mars derived from coordinated analysis of OMEGA (Observatoire pour la Mineralogie, l'Eau, les Glaces et l'Activité) and CRISM (Compact Reconnaissance Imaging Spectrometer for Mars) reflectance observations. We focus on the Syrtis Major-Nili Fossae region in this analysis due to the excellent exposure of crustal rocks and the diversity of mafic igneous compositions previously identified there [9, 10, 11]. For this initial analysis we focus on the pyroxene mineralogy.

Datasets and Methods: CRISM is a visible-near infrared (VNIR) and infrared (IR) imaging spectrometer on the Mars Reconnaissance Orbiter (MRO) that can acquire high resolution targeted observations at 544 wavelengths from 0.36-3.92 μm at 15-19 m/pixel and multispectral mapping data with 72 wavelengths at 100-200 m/pixel. Observations are processed to account for all instrumental effects and reduced to radiance. From these data, I/F is calculated and then corrected for solar incidence angle and the effects of atmospheric transmission absorptions using an approach similar to that used by the OMEGA experiment [9]. The transmission spectrum is derived from a CRISM observation across Olympus Mons.

OMEGA is a VNIR and IR hyperspectral imager on the ESA/Mars Express mission [12]. It has a 1.2 mrad IFOV, a spatial sampling that varies from 300 m (at pericenter) to 4.8 km (at 4000 km altitude), and a 7 to 20 nm spectral resolution in 352 spectral bands over 0.35-5.1 μm. Since entering orbit in January 2004, OMEGA has acquired global coverage between 1-2 km/pixel and high resolution (<500 m/pixel) coverage for >5% of the planet.

Pyroxenes exhibit diagnostic absorption bands in the visible-NIR that result from electronic crystal field transitions of Fe in octahedral coordination [13]. The position, strength and shape of the absorptions are a function of the crystal structure and mineral chemistry [14, 15]. Pyroxenes [$(Ca,Fe,Mg)_2Si_2O_6$] are characterized by the presence of two distinct absorptions centered near 1 and 2 μm. The band centers shift towards longer wavelengths with increasing calcium content. High calcium pyroxenes (e.g. clinopyroxene) typically have long wavelength band centers (1.05 and 2.3 μm) while low calcium pyroxenes (e.g. orthopyroxene) have short wavelength band centers (0.9 and 1.8 μm) [14].

To map the distribution of pyroxene, we use a method based on the Modified Gaussian Model [4]. For the OMEGA data we use the Short Wavelength InfraRed (SWIR, 1.0-2.6 μm) wavelength range to avoid problems due to discrepancies in the spectra at the overlap between two detectors. Similary for the CRISM data we only use the 1.0-2.6 μm wavelength region. In addition, we focus exclusively on multispectral mapping strips for the CRISM data. The multispectral mapping strips provide the best resolution for joint analysis with OMEGA. We use a linear continuum, which is justified by the fits presented in [16] where the continuum is very close to linearity in the wavelength range considered here. We use two gaussians at 1.9 and 2.3 μm with a FWHM of 0.5 and 0.56 μm in agreement with [3], representing LCP and HCP bands respectively. A third absorption band centered at 0.95 μm with a 0.4 μm width is used to constrain the fits and allow convergence of the solutions. While pyroxenes have distinct 1.0 μm bands, the instruments (CRISM and OMEGA) switch detectors near 1.0 μm, causing discontinuities in the spectra. Thus the wavelength region analyzed is not sufficient to constrain the full band shape. Furthermore the presence of numerous overlapping absorptions from pyroxene, olivine, and ferric mineals leads to results that are not unique and thus have no physical significance in the wavelength range of study. We further constrain the fitting algorithm by fixing the band positions and widths. In essence we

are only fitting the pyroxene absorptions at 2.0 μm. The validity of this approximately has been checked empirically by applying the algorithm with all the parameters free on OMEGA data of the Syrtis Major area. The results are very consistent between the contrained and free cases. [7, 8].

Results: In Figure 1 is shown the results of pyroxene mapping for the region. This illustrates the strengths of OMEGA data for establishing regional compositional properties and for CRISM in highlighting local geologic environments. It is very evident in Figure 1 that the Noachain highlands in this region are enriched in LCP relative to the Hesperian-aged volcanic plains of Syrtis Major. We also compute the normalized band strength ratio for LCP given by

$$NBSR_{LCP} = BS_{LCP} / (BS_{LCP} + BS_{HCP})$$

where $NBSR_{LCP}$ is the normalized band strength ratio for LCP, BS_{LCP} is the band strength of LCP from the MGM model, and BS_{HCP} is the band strength of HCP from the MGM model. This ratio has been shown to be linearly related to the relative proportions of LCP and HCP in pyroxene mixtures with an accuracy of +/-10% [18]. This is given in Figure 2 for the same region.

The mapping with CRISM data consistently agrees with OMEGA mapping despite the differences in instruments. Yet there appears to be a systematic increase in the calculated HCP concentration returned by CRISM. This is possibly due to the CRISM atmosheric removal which may remove too much water vapor causing an apparent absorption band near 2.5 μm.

Together with Figure 1, it is clear that there is an apparent enrichment of LCP in the Noachian-aged highlands in this region. This is in agreement with previous work [9, 10]. We gathered statistics for the portions of the regions enriched in LCP and those in HCP. We find that LCP regions show a NBSR of 0.6+/-0.08 and the HCP regions show 0.4+/-0.05. These differences exceed the uncertainties according to the analytical work of [18] and thus the highlands show about a 20% increase in the relative proportion of LCP compared to the volcanic plains of Syrtis Major.

It is also interesting to note that the Noachian highlands show a higher degree of variance than the volcanic plains. This was observed in some of the high resolution observations of OMEGA but is revealed with greater spatial continuity in the CRISM data. Values of NBSR as high as and exceeding 0.8 are observed in the CRISM data. Some of this high variance is observed at the pixel scale (200 m) of CRISM. In constrast, compositional variation in pyroxene content for the Syrtis Major lava plains is much less.

The presence of HCP enrichment in the ejecta deposits of some of the craters in Syrtis Major was analyzed by [19]. They argue that this could be due to the presence of HCP-enriched lava flows at depth. Modeling suggests a depth of 300 m. The enrichment of HCP in some ejecta blankets is confirmed by CRISM. Full resolution CRISM observations reveal interesting details of the geology, including excavation of HCP-enriched rocks from beneath a cover of LCP-enriched materials and the complex nature of the Noachian Highland (Figure 3). The $NBSR_{LCP}$ shows values in excess of 0.8 but also show high variability over short length scales. In this region the absence of mafic mineral detections are associated with the presence of phyllosilicate minerals.

Conclusions: There is a clear and statistically significant difference in the relative pyroxene content of the Noachian highlands relative to the Hesperian-aged lavas of Syrtis Major. While it is not yet possible to quantify the total modal amount of pyroxene in these regions, based on TES and radiative transfer modeling of OMEGA data, we broadly estimate between 20 and 40% pyroxene. The MGM modeling clearly shows that the Noachain highlands have a 60:40 ratio of LPC:HCP, while the volcanic plains are the opposite, 40:60. We are currently analyzing possible models to explain this difference.

It is very evident that the Noachian-aged terrains show a much greater variance in pyroxene composition than the lava plains. This can be observed at the spatial resolution of CRISM (200 m/pixel) and shows a great deal of spatial complexity. The complexity shown in this region of Noachian crust would be consistent with layered materials reworked and redistributed by impacts of different sizes, including basin-forming events.

References: [1] McSween, H. Y. et al. (2003), JGR 108, 10.1029/2003JE002175. [2] Bandfield, J. L. et al. (2000), Science 287, 1626. [3] Mustard, J. F. et al. (1997), JGR 102, 25605-25616. [4] Hamilton, V. E. et al. (2001), JGR 106, 14733. [5] Wyatt, M. B., McSween, H. Y. (2002), Nature 417, 263. [6] Morris, R. V. et al. (2003), Sixth International Conference on Mars, LPI Contribution 3211. [7] Minitti, M. E. et al. (2002), JGR 107, E5, 10.1029. [8] Kraft, M. D., Michalski, J. R., Sharp, T. G. (2003), Geophys. Res. Let. 30, Art. No. 2288. [9] Bibring, J-P. et al. (2005), Science 307, 1576-1581. [10] Mustard, J. F. et al. (2005), Science 307, 1594-1597. [11] Bandfield, J. L. (2002), JGR 107, E6 5042. [12] Bibring, J-P. et al. (2004), *ESA SP 1240*, 37. [13] Burns, R. G., Mineralogic Applications of Crystal Field Theory, Cambridge University Press 1970. [14] Adams, J. B. (1974), JGR 79, 4829. [15] King, T. V. V., Ridley, I. (1987), JGR 92, 11457. [16] Sunshine et al. (1990), JGR 95, 6955-6966. [17] Gendrin A. et al. (2006), LPSC. [18] Kanner, L. C. et al. (2007), Icarus 187, 2, 442-456. [19] Baratoux et al., this issue.

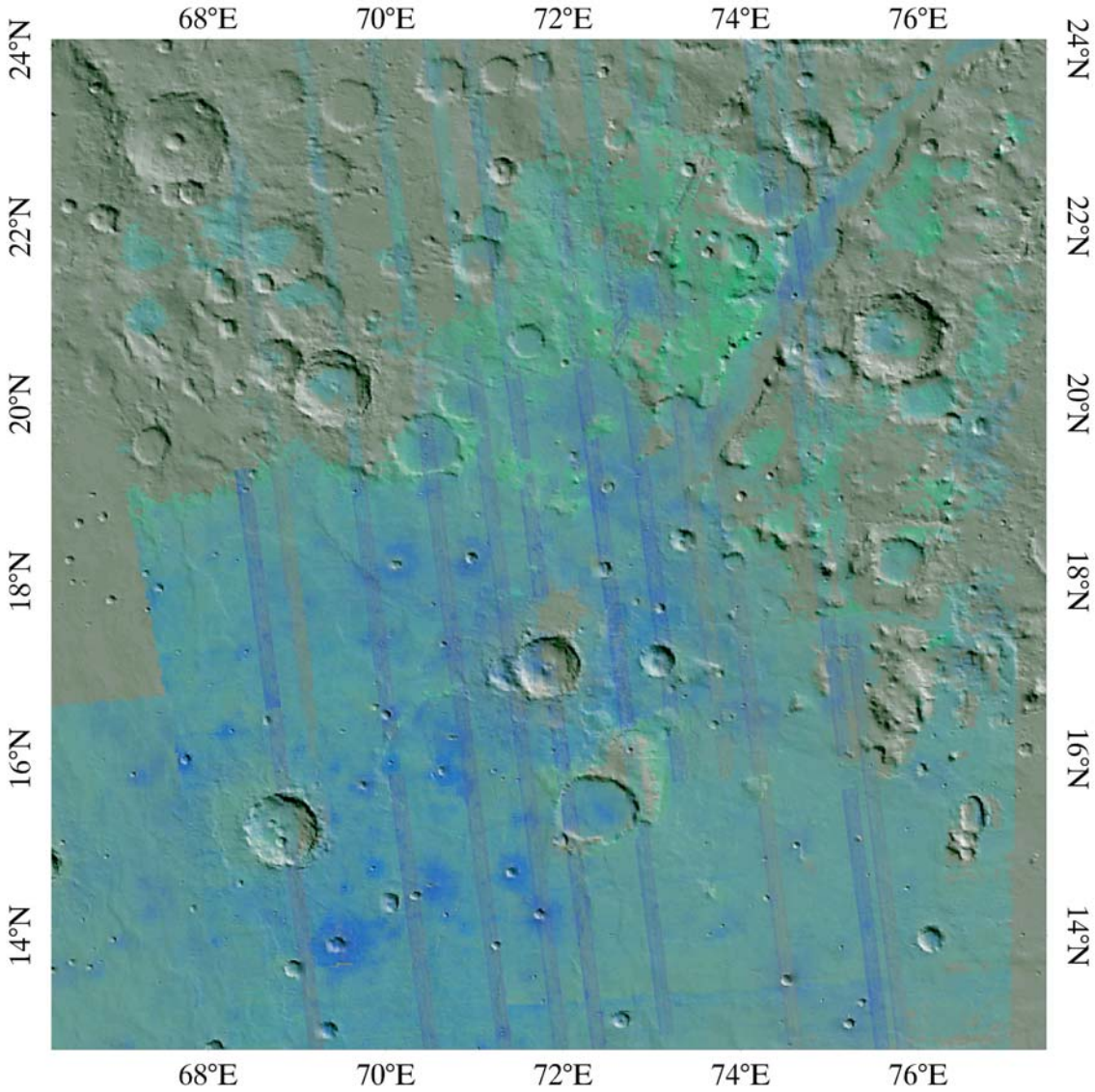

Figure 1. Strength of pyroxene absorption bands from OMEGA and CRISM data in the Syrits Major-Nili Fossae region. LCP band strength is shown in green and HCP band strength in blue. OMEGA data provide a regional coverage while CRISM multispectral mapping data are shown in the narrow strips across the scene.

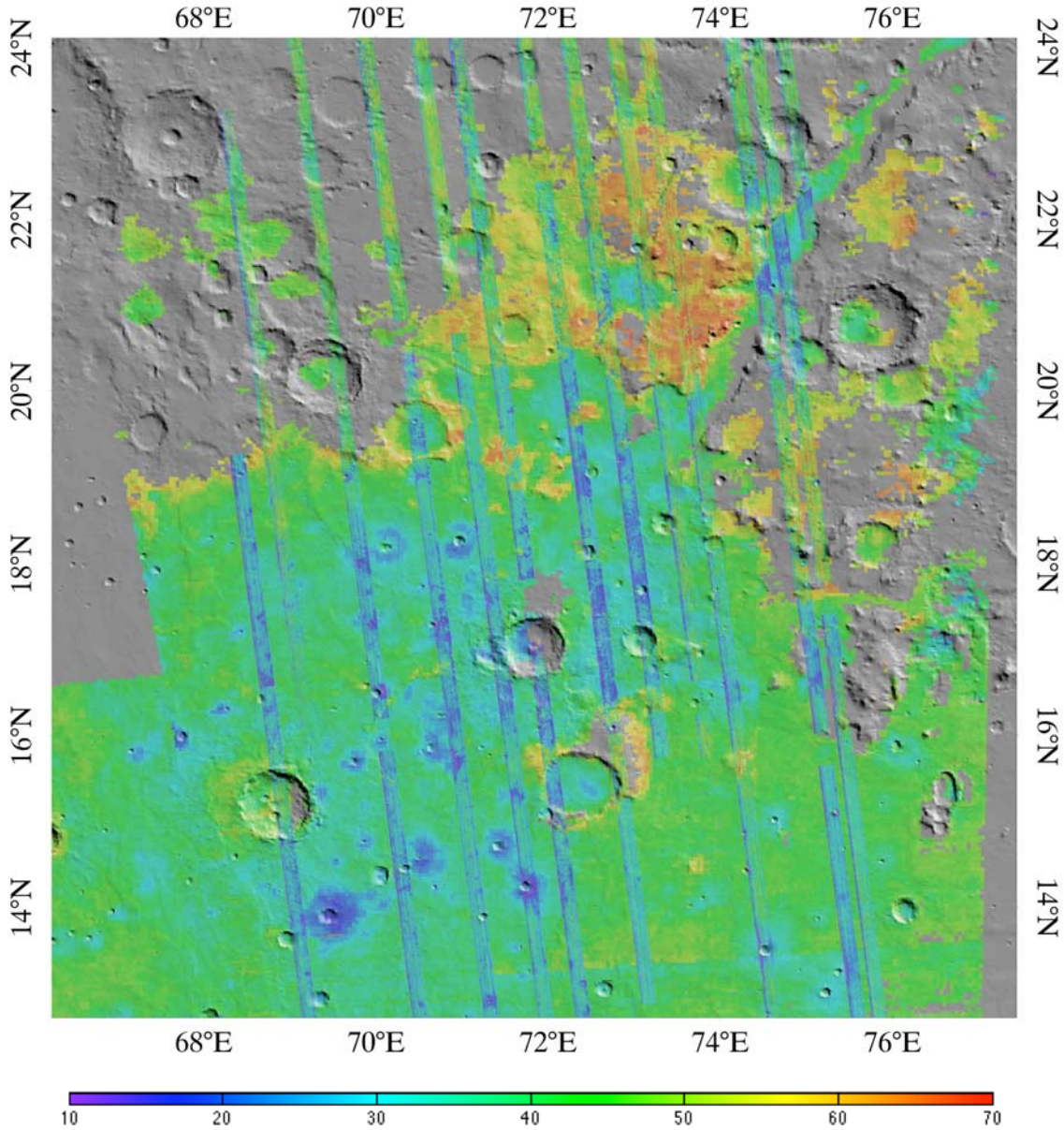

Figure 2. Normalized Band Strength Ratio for Low Calcium Pyroxene. The color scale runs from 10% LCP:HCP for pure blue colors to 70% LCP:HCP for the pure red colors. The intermediate green tones across the Syrtis Major plains have a value near 40% LCP:HCP.

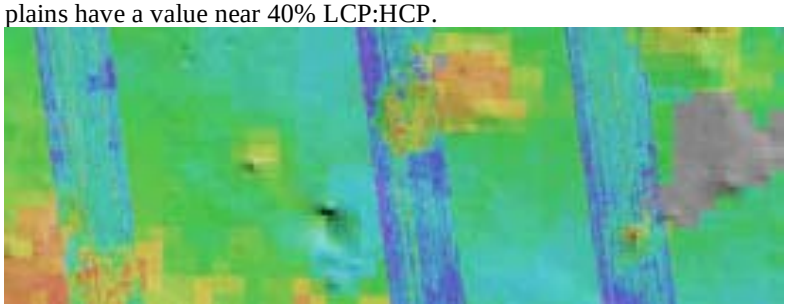

Figure 3. Full resolution view of $NBSR_{LCP}$. Note the very high values (>0.8) in the highland massifs surrounded by Syrtis Major lavas.